PAPER

Single-Carrier Multi-User MIMO Downlink with Time-Domain Tomlinson-Harashima Precoding

Shohei YOSHIOKA[†a)], **Shinya KUMAGAI**[†], *Student Members*, *and* **Fumiyuki ADACHI**[†], *Fellow*

SUMMARY Nonlinear precoding improves the downlink bit error rate (BER) performance of multi-user multiple-input multiple-output (MU-MIMO). Broadband single-carrier (SC) block transmission can improve the capability that nonlinear precoding reduces BER, as it provides frequency diversity gain. This paper considers Tomlinson-Harashima precoding (THP) as a nonlinear precoding scheme for SC-MU-MIMO downlink. In the SC-MU-MIMO downlink with frequency-domain THP proposed by Degen and Rrühl (called SC-FDTHP), the inter-symbol interference (ISI) is suppressed by transmit frequency-domain equalization (FDE) after suppressing the inter-user interference (IUI) by frequency-domain THP. Transmit FDE increases the signal variance, hence transmission performance improvement is limited. In this paper, we propose a new SC-MU-MIMO downlink with time-domain THP which can pre-remove both ISI and IUI (called SC-TDTHP) if perfect channel state information (CSI) is available. Modulo operation in THP suppresses the signal variance increase caused by ISI and IUI pre-removal, and hence the transmission quality improves. For further performance improvement, vector perturbation is introduced to SC-TDTHP (called SC-TDTHP w/VP). Computer simulation shows that SC-TDTHP achieves better BER performance than SC-FDTHP and that SC-TDTHP w/VP offers further improvement in BER performance over SC-MU-MIMO with VP (called SC-VP). Computational complexity is also compared and it is showed that SC-TDTHP and SC-TDTHP w/VP incur higher computational complexity than SC-FDTHP but lower than SC-VP.
key words: *MU-MIMO, Tomlinson-Harashima precoding, single-carrier downlink, time-domain, vector perturbation*

1. Introduction

Multi-user multiple-input multiple-output (MU-MIMO) [1]–[13] is a promising space-division multiple access (SDMA) technique. In MU-MIMO, a base station (BS) having multiple antennas communicates with multiple users using the same frequency without expanding frequency bandwidth. In general, users cannot know the other users' channel state information (CSI). For MU-MIMO downlink transmissions, precoding is employed [3]–[6] at the transmitter, i.e. BS, in order to suppress inter-user interference (IUI). MU-MIMO downlink with precoding may exhibit worse bit error rate (BER) performance than that of MU-MIMO uplink employing a maximum likelihood detection technique [7], [8]. According to [9], nonlinear precoding schemes achieve better BER performance than linear precoding schemes. It is expected that nonlinear precoding will improve the MU-MIMO downlink BER performance.

In broadband single-carrier (SC) block transmission with compensation of the spectrum distortion caused by the channel's frequency-selectivity [14], [15], the nonlinear precoding schemes are capable of improving further the BER performance as it provides frequency diversity gain. In this paper, we consider Tomlinson-Harashima precoding (THP) [5] for SC-MU-MIMO. The original THP pre-removes the IUI by successive subtraction and precoding matrix multiplication (this can be done by making the equivalent channel matrix representing a product of a channel matrix and the precoding matrix to be a triangular matrix). Although the successive IUI subtraction increases the variance of the signal, THP suppresses the increase of the variance by modulo operation after each stage of the successive subtraction. By normalizing the signal power after THP, the received signal-to-noise power ratio (SNR) improves compared to that with a linear precoding scheme.

For SC-MU-MIMO downlink with THP, it is necessary to suppress the inter-symbol interference (ISI) caused by the channel frequency-selectivity as well as IUI. ISI pre-removal at the BS transmitter is feasible since BS is able to know the equivalent channel matrix including CSIs associated with all of users in communication. In the study about SC-MU-MIMO downlink with THP proposed by Degen and Rrühl (called SC-FDTHP) [10], transmit frequency-domain equalization (FDE) is carried out to suppress the ISI after IUI subtraction in frequency-domain THP. The IUI and ISI pre-removal operation increases the signal variance. Although the modulo operation in SC-FDTHP suppresses the signal variance increase caused by the IUI pre-removal, the signal variance increase caused by the ISI pre-removal remains. Consequently, SC-FDTHP provides only slight received SNR improvement compared to linear precoding schemes. Note that if performing transmit FDE before THP, the signal constellation has an extremely large number of signal points and therefore, it is difficult to determine the divisor in modulo operation.

First in this paper, we propose a new SC-MU-MIMO with time-domain THP for both IUI and ISI pre-removal (SC-TDTHP). In SC-TDTHP, ISI as well as IUI is simultaneously pre-removed by time-domain THP. Modulo operation in SC-TDTHP can suppress the signal variance increase caused by ISI pre-removal, which is a major difference from SC-FDTHP.

Next in this paper, we propose SC-TDTHP combined with vector perturbation [6] (SC-TDTHP w/VP). As with SC-MU-MIMO with VP (SC-VP) [11], M algorithm based perturbation vector search is applied to reduce the compu-

Manuscript received April 14, 2015.
Manuscript revised September 14, 2015.
[†]The authors are with the Department of Communications Engineering, Graduate School of Engineering, Tohoku University, Sendai-shi, 980-8579 Japan.
a) E-mail: yoshioka@mobile.ecei.tohoku.ac.jp
DOI: 10.1587/transcom.2015EBT0001

tational complexity of SC-TDTHP w/VP. In addition, interleaving before THP and de-interleaving after THP at the transmitter are applied to improve the accuracy of the perturbation vector search by M algorithm. The extended channel matrix in SC-TDTHP is a sparse matrix, and hence the interleaving generates zero elements in triangular part of the equivalent channel matrix [16], [17].

The remainder of this paper is organized as follows. Section 2 proposes SC-TDTHP and Sect. 3 proposes SC-TDTHP w/VP. Section 4 provides computer simulation results. Computational complexity comparison among SC-TDTHP, SC-TDTHP w/VP, SC-FDTHP, and SC-VP is provided in Sect. 5. Finally, Sect. 6 concludes the paper.

In this paper, it is shown that SC-TDTHP achieves better BER performance than SC-FDTHP, by computer simulation. Also shown is that coded BER performance of SC-TDTHP is slightly better than that of orthogonal frequency-domain multiplexing MU-MIMO with THP (OFDM-THP). We show that SC-TDTHP w/VP achieves better BER performance than SC-VP, by applying interleaving. Computational complexities of SC-TDTHP and SC-TDTHP w/VP are compared to those of SC-FDTHP and SC-VP.

In this paper, we assume cyclic prefix (CP) inserted block transmission and a BS communicates with U users simultaneously. The BS has N_T transmit antennas and users have the single receive antenna. We define $[.]^T$ as the transpose operator, $[.]^H$ as the Hermitian transpose operator, and $||.||$ as the Euclidean norm of the vector.

2. SC-TDTHP

In this section, we propose SC-TDTHP. Transmitter/receiver structures are illustrated in Fig. 1. THP for IUI/ISI pre-removal is performed in time-domain. To pre-remove IUI/ISI by THP, SC-TDTHP expresses all users' symbol blocks as a $UN_c \times 1$ vector and applies precoding to the vector, using an extended channel matrix taking account of multiple delayed paths, where UN_c is the block size. The

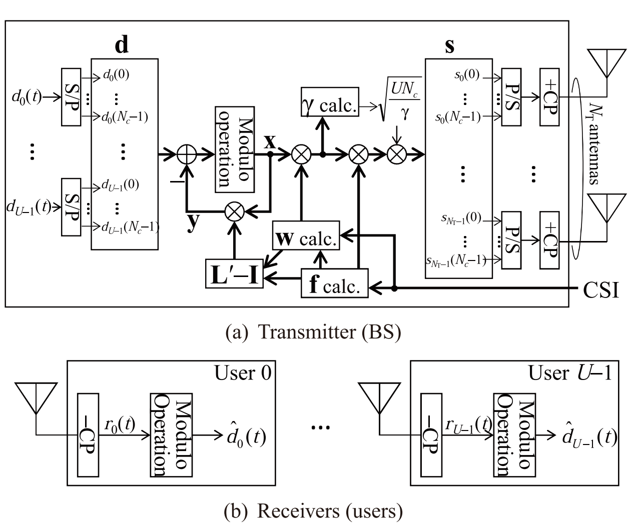

Fig. 1 Transmitter/receivers structures of SC-TDTHP.

$UN_c \times N_TN_c$ extended channel matrix h is represented as

$$\mathbf{h} = \begin{pmatrix} \mathbf{h}_{00} & \cdots & \mathbf{h}_{0(N_T-1)} \\ \vdots & \ddots & \vdots \\ \mathbf{h}_{(U-1)0} & \cdots & \mathbf{h}_{(U-1)(N_T-1)} \end{pmatrix}, \tag{1}$$

with

$$\mathbf{h}_{un_T} = \begin{pmatrix} h_{0,un_T} & & & h_{\Lambda-1,un_T} & \cdots & h_{1,un_T} \\ h_{1,un_T} & h_{0,un_T} & & & \ddots & \vdots \\ \vdots & h_{1,un_T} & \ddots & \mathbf{0} & & h_{\Lambda-1,un_T} \\ h_{\Lambda-1,un_T} & \vdots & \ddots & h_{0,un_T} & & \\ & h_{\Lambda-1,un_T} & & h_{1,un_T} & \ddots & \\ \mathbf{0} & & \ddots & \vdots & \ddots & h_{0,un_T} \end{pmatrix}, \tag{2}$$

being the $N_c \times N_c$ channel impulse response matrix between the u-th user's receive antenna and the n_T-th BS transmit antenna, assuming the time delay of $\lambda(=0\sim\Lambda-1)$-th path $\tau_\lambda=\lambda T_s$. T_s, h_{λ,un_T}, and Λ are the symbol duration, the complex-valued path gain of the λ-th path, and the number of delay paths, respectively. Precoding matrix $\mathbf{f}$ for IUI/ISI subtraction, i.e. transforming the product of the channel matrix and the precoding matrix to a lower triangular matrix, is obtained by applying LQ decomposition [18] to the extended channel matrix $\mathbf{h}$ as

$$\mathbf{h} = \begin{pmatrix}\mathbf{L} & \mathbf{0}\end{pmatrix}\mathbf{Q} = \begin{pmatrix}\mathbf{L} & \mathbf{0}\end{pmatrix}\begin{pmatrix}\mathbf{Q}_L \\ \mathbf{Q}_0\end{pmatrix}, \tag{3}$$

$$\mathbf{f} = \mathbf{Q}_L^H. \tag{4}$$

$\mathbf{L}$ is the lower triangular matrix of order UN_c whose diagonal elements are real numbers. $\mathbf{Q}_L$ and $\mathbf{Q}_0$ correspond to the $0\sim(UN_c-1)$-th and $UN_c\sim(N_TN_c-1)$-th rows of the unitary matrix Q of order N_TN_c, respectively. THP pre-removing IUI/ISI leaves amplitude variation within a received block at a user receiver since the diagonal elements of $\mathbf{hf}=\mathbf{L}$ are not constant. Thus, SC-TDTHP multiplies weight for pre-removing the amplitude variation. The amplitude variation pre-removal increases the variance of the signal; however, the increase is much smaller than that caused by ISI pre-removal in SC-FDTHP. The weight to pre-remove the amplitude variation equalizes all of the diagonal elements of $\mathbf{L}$ to 1 and is calculated as

$$\begin{aligned} \mathbf{w} &= diag\{w_0, \ldots, w_{UN_c-1}\} \\ &= diag\left\{L_{00}^{-1}, \ldots, L_{(UN_c-1)(UN_c-1)}^{-1}\right\}, \end{aligned} \tag{5}$$

where L_{ij}; i, j=0$\sim UN_c-1$, is the (i, j)-th element of $\mathbf{L}$. From Eqs. (3)–(5), the equivalent channel matrix between amplitude variation pre-removal at the BS and CP removal at users is given as

$$\begin{aligned} \mathbf{L}' &= \mathbf{Lfw} \\ &= \begin{pmatrix} L_{00} & & \mathbf{0} \\ \vdots & \ddots & \\ L_{(UN_c-1)0} & \cdots & L_{(UN_c-1)(UN_c-1)} \end{pmatrix} \begin{pmatrix} w_{00} & & \mathbf{0} \\ & \ddots & \\ \mathbf{0} & & w_{UN_c-1} \end{pmatrix} \end{aligned}$$

$$= \begin{pmatrix} 1 & & & \mathbf{0} \\ \frac{L_{10}}{L_{00}} & \ddots & & \\ \vdots & \ddots & \ddots & \\ \frac{L_{(UN_c-1)0}}{L_{00}} & \cdots & \frac{L_{(UN_c-1)(UN_c-2)}}{L_{(UN_c-2)(UN_c-2)}} & 1 \end{pmatrix}. \quad (6)$$

Precoding in SC-TDTHP is performed using $\mathbf{L}'$, $\mathbf{w}$, and $\mathbf{f}$.

The $UN_c \times 1$ vector representing time-domain data-modulated symbol blocks $\{d_u(t); t = 0{\sim}N_c-1\}$, $u = 0{\sim}U-1$, is written as $\mathbf{d} = [d_0(0) \ldots d_0(N_c-1) \ldots d_{U-1}(0) \ldots d_{U-1}(N_c-1)]^T$. The i $(= 0 \sim UN_c \times 1)$-th element in $\mathbf{d}$ is expressed as d_i. The BS performs the following IUI/ISI subtraction and modulo operation to $\mathbf{d}$ successively in order of $d_0, d_1, \ldots, d_{UN_c-1}$. IUI/ISI are subtracted from d_i and symbol a_i after IUI/ISI subtraction is given as

$$a_i = d_i - y_i, \quad (7)$$

where y_i is the IUI/ISI for d_i. Modulo operation to the real and imaginary parts of a_i, i.e.

$$\begin{aligned} x_i &= (a_i)\mathrm{mod}\tau \\ &:= a_i + \tau z_i, \end{aligned} \quad (8)$$

suppresses the signal variance increase caused by IUI/ISI pre-removal of Eq. (7). τ depends on the modulation level and $\tau{=}2\sqrt{2}$ in QPSK. For later calculation, the real and imaginary parts of z_i are integer. Vector expressions of a_i, x_i, y_i, and z_i, $i{=}0{\sim}UN_c{-}1$ are represented as $\mathbf{a}{=}[a_0 \ldots a_{UN_c-1}]^T$, $\mathbf{x}{=}[x_0 \ldots x_{UN_c-1}]^T$, $\mathbf{y}{=}[y_0 \ldots y_{UN_c-1}]^T$, and $\mathbf{z}{=}[z_0 \ldots z_{UN_c-1}]^T$, respectively.

After the above successive IUI/ISI subtraction and modulo operation, the BS pre-removes the amplitude variation by multiplying $\mathbf{w}$. Then, the precoding matrix $\mathbf{f}$ is multiplied and the signal power is normalized as

$$\mathbf{s} = \sqrt{\frac{UN_c}{\gamma}}\mathbf{fwx}. \quad (9)$$

The $N_T N_c \times 1$ vectors $\mathbf{s}{=}[s(0) \ldots s(N_T N_c{-}1)]^T$ has the N_T symbol blocks and $\{s(n_T N_c{+}t);\ t{=}0{\sim}N_c{-}1\}$, $n_T{=}0{\sim}N_T{-}1$ in $\mathbf{s}$ is the transmit symbol block from the n_T-th transmit antenna. The power normalization coefficient γ keeps the transmit power constant as

$$\begin{aligned} \gamma &= \|\mathbf{fwx}\|^2 \\ &= \|\mathbf{w}(\mathbf{a} + \tau\mathbf{z})\|^2. \end{aligned} \quad (10)$$

After inserting a CP of N_g symbols into the guard interval (GI), the BS transmits symbol blocks from N_T transmit antennas.

Consequently, y_i for pre-removing IUI/ISI perfectly can be calculated. Pre-removing IUI/ISI perfectly is equivalent to

$$\mathbf{L}'\mathbf{x} = \mathbf{d} + \tau\mathbf{z}. \quad (11)$$

y_i is obtained from Eq. (11) as

$$y_i = \begin{cases} 0 & \text{for } i = 0 \\ \displaystyle\sum_{j=0}^{i-1} \frac{L_{ij}}{L_{jj}} x_j & \text{for } i > 0 \end{cases}. \quad (12)$$

Each user receives the symbol block, and then removes the CP from the received block. When the received symbol blocks $\{r_u(t);\ t{=}0{\sim}N_c{-}1\}$, $u{=}0{\sim}U{-}1$, after CP removal are written as the $UN_c \times 1$ vector $\mathbf{r}{=}[r_0(0) \ldots r_0(N_c{-}1) \ldots r_{U-1}(0) \ldots r_{U-1}(N_c{-}1)]^T$, $\mathbf{r}$ is given as

$$\begin{aligned} \mathbf{r} &= \sqrt{\frac{2E_s}{T_s}}\mathbf{hs} + \mathbf{n} \\ &= \sqrt{\frac{2E_s}{T_s}\frac{UN_c}{\gamma}}\mathbf{hfw}(\mathbf{d} - \mathbf{y} + \tau\mathbf{z}) + \mathbf{n} \\ &= \sqrt{\frac{2E_s}{T_s}\frac{UN_c}{\gamma}}\mathbf{L}'(\mathbf{d} - \mathbf{y} + \tau\mathbf{z}) + \mathbf{n} \\ &= \sqrt{\frac{2E_s}{T_s}\frac{UN_c}{\gamma}}(\mathbf{d} + \tau\mathbf{z}) + \mathbf{n}, \end{aligned} \quad (13)$$

where E_s is the average transmit symbol energy. $\mathbf{n}{=}[n_0 \ldots n_{UN_c-1}]^T$ is the $UN_c \times 1$ noise vector whose elements are the complex Gaussian variables having zero mean and variance $2\sigma^2{=}2N_0/T_s$ with N_0 being the single-sided power spectrum density of additive white Gaussian noise (AWGN). Each receiver does not require CSI and divides the received block by the desired symbol coefficient of Eq. (13) (the first coefficient of the right side). After modulo operation to remove $\tau\mathbf{z}$, data demodulation is done. When turbo coding and QPSK are used, the bit log-likelihood ratio (LLR) is computed for the b(=0 or 1)-th bit as

$$\mathrm{LLR}_u(t,b) = \frac{1}{2\sigma^2}\left(\left| r_u(t) - \sqrt{\frac{2E_s}{T_s}\frac{UN_c}{\gamma}}\xi_{0,\min} \right|^2 - \left| r_u(t) - \sqrt{\frac{2E_s}{T_s}\frac{UN_c}{\gamma}}\xi_{1,\min} \right|^2 \right), \quad (14)$$

where $\xi_{0,\min}$ or $\xi_{1,\min}$ are the candidate symbols having the b-th bit=0 and 1, respectively, which give the minimum Euclidean distance from $r_u(t)$.

Note that user ordering is not applied to basic SC-TDTHP proposed in this section. However, similar to SC-FDTHP [10], an application of user ordering like [13] to SC-TDTHP may further improve the transmission performance of SC-TDTHP. To confirm the effectiveness of user ordering, the BER performance of SC-TDTHP with simple user ordering is also evaluated in Sect. 4.

3. SC-TDTHP w/VP

Modulo operation of Eq. (8) suppresses the signal variance increase caused by the previous IUI/ISI subtraction of

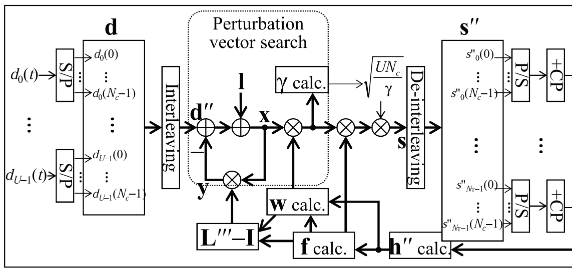

Fig. 2 Transmitter structure of SC-TDTHP w/VP.

Eq. (7). Modulo operation in THP cannot take account of the signal variance increase caused by the entire precoding operation. Note that modulo operation after the interference subtraction is equivalent to adding an auxiliary vector in order to shift the symbol position in the signal space near the original constellation. The auxiliary vector can be regarded as a kind of perturbation vector in VP. VP can suppress the signal variance increase caused by the entire precoding operation. The optimal perturbation vector in SC-TDTHP as VP is capable of suppressing the signal variance increase more and improves the received SNR.

In this section, we combine SC-TDTHP with VP instead of modulo operation for further improvement of transmission performance. Figure 2 shows transmitter structure of SC-TDTHP w/VP. Receivers structures are the same as those of SC-TDTHP. The flow of signal processing at BS is based on the previous section, and only modified processing is discussed in this section.

3.1 M Algorithm Based Perturbation Vector Search

SC-TDTHP suppresses the signal variance increase by modulo operation. z_i in Eq. (8) minimizes the signal variance of x_i, which includes $x_0 \sim x_{i-1}$. However, each modulo operation does not take account of the latter signal processing. In SC-TDTHP w/VP, the modulo operation is replaced to perturbation vector addition, hence Eq. (8) is rewritten as

$$x_i = a_i + \tau l_i, \tag{15}$$

where l_i is the i-th element in the $UN_c \times 1$ perturbation vector $\mathbf{l}=[l_0 \dots l_{UN_c-1}]^T$ whose element has the real and imaginary part of integral. The power normalization coefficient is rewritten from Eq. (10) to

$$\begin{aligned}\gamma &= \|\mathbf{wx}\|^2\\ &= \|\mathbf{w}(\mathbf{a}+\tau\mathbf{l})\|^2.\end{aligned} \tag{16}$$

Ideally, the perturbation vector $\mathbf{l}$ is determined based on

$$\begin{aligned}\mathbf{l} &= \arg\min_{\mathbf{l}'} \gamma\\ &= \arg\min_{\mathbf{l}'} \left(\left\| \mathbf{w}(\mathbf{a}+\tau\mathbf{l}') \right\|^2 \right),\end{aligned} \tag{17}$$

though the perturbation vector has the extremely large number K^{UN_c} of candidates, where K denotes the number of candidates for each element of the perturbation vector. The number of perturbation vector candidates is the same as that of SC-VP. When we set K=9, U=4, and N_c=64, for example, $K^{UN_c}=9^{4\times 64}\approx 2\times 10^{244}$. Thus, the optimal perturbation vector cannot be found realistically due to the huge computational complexity.

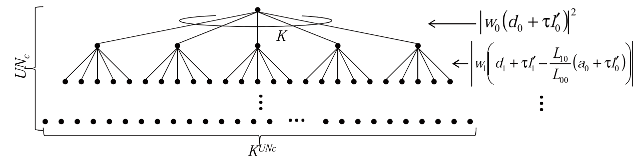

Fig. 3 Tree structure of Eq. (18) when K=5.

In SC-TDTHP w/VP, IUI/ISI subtraction and perturbation vector addition are performed successively. Eq. (17) is written as

$$\mathbf{l} = \arg\min_{\mathbf{l}'} \left(\begin{array}{l} \left|w_0\left(d_0+\tau l_0'\right)\right|^2 + \\ \left|w_1\left(d_1+\tau l_1'-\dfrac{L_{10}}{L_{00}}\left(a_0+\tau l_0'\right)\right)\right|^2 + \\ \cdots + \\ \left| w_{UN_c-1} \left(\begin{array}{l} d_{UN_c-1}+\tau l_{UN_c-1}' \\ -\displaystyle\sum_{j=0}^{UN_c-2} \dfrac{L_{(UN_c-1)j}}{L_{jj}}\left(a_j+\tau l_j'\right) \end{array} \right) \right|^2 \end{array} \right), \tag{18}$$

In SC-VP, M algorithm is applied for reducing the computational complexity after QR decomposition [12]. On the other hand, the perturbation vector search of Eq. (18) can be expressed as a tree structure of ascending order of the elements in $\mathbf{l}$, as shown in Fig. 3. Thus, SC-TDTHP w/VP searches a near-optimal perturbation vector using M algorithm directly for computational complexity reduction, following SC-VP. Eq. (18) shows that perturbation vector search by M algorithm is performed subtracting IUI/ISI and pre-removing the amplitude variation. When M denotes the number of the candidates kept at each stage in M algorithm, the number of perturbation vector search candidates becomes about $MKUN_c$. M algorithm can sufficiently reduce the computational complexity for perturbation vector search. For example, in using the former parameters and M=50, $MKUN_c$=115200.

3.2 Interleaving and De-Interleaving at BS

Accuracy of perturbation vector search based on M algorithm depends on how much a stage in the tree structure is affected by the previous stages. When the effect is larger, low accuracy at a stage degrades that at the following stages. In other words, smaller magnitudes of non-diagonal elements in the equivalent channel matrix $\mathbf{L'}$ provide higher accuracy of the perturbation vector search based on M algorithm. Since the extended channel matrix $\mathbf{h}$ in SC-TDTHP

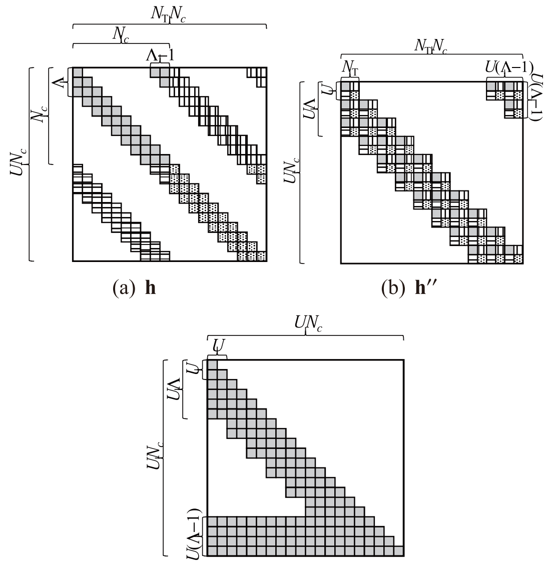

(a) $\mathbf{h}$ (b) $\mathbf{h}''$

(c) $\mathbf{L}''$ and $\mathbf{L}'''$

Fig. 4 Outline of each matrix (U=N_T=2, Λ=3, N_c=10).

w/VP has sparseness, the smallest magnitudes, i.e. zeros, can be generated intentionally. After rearrangement of

$$\mathbf{h}'' = \mathbf{M}^T\mathbf{h}\mathbf{N}, \tag{19}$$

and LQ decomposition to $\mathbf{h}''$ of

$$\mathbf{h}'' = \begin{pmatrix}\mathbf{L}'' & \mathbf{0}\end{pmatrix}\mathbf{Q}'' = \begin{pmatrix}\mathbf{L}'' & \mathbf{0}\end{pmatrix}\begin{pmatrix}\mathbf{Q}''_L \\ \mathbf{Q}''_0\end{pmatrix}, \tag{20}$$

the lower triangular matrix $\mathbf{L}''$ has zeros as shown in Fig. 4. $\mathbf{M}$=$[(\boldsymbol{\alpha}_0\boldsymbol{\alpha}_{N_c}\ldots\boldsymbol{\alpha}_{(U-1)N_c})\ldots(\boldsymbol{\alpha}_{N_c-1}\boldsymbol{\alpha}_{2N_c-1}\ldots\boldsymbol{\alpha}_{UN_c-1}]$ and $\mathbf{N}$=$[(\boldsymbol{\beta}_0\boldsymbol{\beta}_{N_c}\ldots\boldsymbol{\beta}_{(N_T-1)N_c})\ldots(\boldsymbol{\beta}_{N_c-1}\boldsymbol{\beta}_{2N_c-1}\ldots\boldsymbol{\beta}_{N_TN_c-1}]$ denote an interleaving matrix of order UN_c and a de-interleaving matrix of order N_TN_c when $\boldsymbol{\alpha}_i$ and $\boldsymbol{\beta}_i$ represent a $UN_c \times 1$ and a $N_TN_c \times 1$ unit vector (whose i-th element is 1 and the others are 0), respectively. Therefore, SC-TDTHP w/VP applies interleaving and de-interleaving so that the equivalent channel matrix including $\mathbf{L}''$ is used for IUI/ISI subtraction in THP. Note that it is impossible to interleave symbols among users in general. Both of interleaving and de-interleaving should be performed at BS. It is also noted that since interleaving rearranges input symbols in the same order always, no matrix multiplication is required.

The UN_c×1 vector $\mathbf{d}$ representing data-modulated symbol blocks is interleaved as

$$\mathbf{d}'' = \mathbf{M}^T\mathbf{d}. \tag{21}$$

The de-interleaving is performed to the $N_TN_c \times 1$ vector $\mathbf{s}$ of Eq. (9) as

$$\mathbf{s}'' = \mathbf{N}\mathbf{s}. \tag{22}$$

From the above rearrangements, the $UN_c \times 1$ vector $\mathbf{r}$ representing received symbol blocks is given as

$$\begin{aligned}\mathbf{r} &= \sqrt{\frac{2E_s}{T_s}}\mathbf{h}\mathbf{s}'' + \mathbf{n} \\ &= \sqrt{\frac{2E_s}{T_s}}\mathbf{M}\mathbf{h}''\mathbf{N}^T\mathbf{N}\mathbf{s} + \mathbf{n} \\ &= \sqrt{\frac{2E_s}{T_s}\frac{UN_c}{\gamma}}\mathbf{M}\mathbf{h}''\mathbf{f}\mathbf{w}\left(\mathbf{d}'' - \mathbf{y} + \tau\mathbf{l}\right) + \mathbf{n}.\end{aligned} \tag{23}$$

Thus, the rearrangement of Eq. (22) permits precoding using $\mathbf{h}''$.

For the rearranged channel matrix $\mathbf{h}''$, the precoding matrix and the weight for amplitude variation pre-removal are calculated as

$$\mathbf{f} = \mathbf{Q}_L''^H, \tag{24}$$

$$\mathbf{w} = diag\left\{L_{00}''^{-1}, \ldots, L_{(UN_c-1)(UN_c-1)}''^{-1}\right\}, \tag{25}$$

instead of Eqs. (4) and (5), respectively. From Eqs. (20), (24), and (25), the equivalent channel matrix between amplitude variation pre-removal at the BS and CP removal at users is given as

$$\begin{aligned}\mathbf{L}''' &= \mathbf{h}''\mathbf{f}\mathbf{w} \\ &= \mathbf{L}''\mathbf{w} \\ &= \begin{pmatrix} 1 & & & \mathbf{0} \\ \frac{L''_{10}}{L''_{00}} & \ddots & & \\ \vdots & \ddots & \ddots & \\ \frac{L''_{(UN_c-1)0}}{L''_{00}} & \cdots & \frac{L''_{(UN_c-1)(UN_c-2)}}{L''_{(UN_c-2)(UN_c-2)}} & 1 \end{pmatrix}.\end{aligned} \tag{26}$$

y_i for IUI/ISI pre-removal is obtained as not Eq. (12) but

$$y_i = \begin{cases} 0 & \text{for } i = 0 \\ \displaystyle\sum_{j=0}^{i-1}\frac{L''_{ij}}{L''_{jj}}x_j & \text{for } i > 0 \end{cases}. \tag{27}$$

Consequently, Eq. (23) becomes

$$\begin{aligned}\mathbf{r} &= \sqrt{\frac{2E_s}{T_s}\frac{UN_c}{\gamma}}\mathbf{M}\mathbf{L}'''\left(\mathbf{d}'' - \mathbf{y} + \tau\mathbf{l}\right) + \mathbf{n} \\ &= \sqrt{\frac{2E_s}{T_s}\frac{UN_c}{\gamma}}\mathbf{M}\left(\mathbf{d}'' + \tau\mathbf{l}\right) + \mathbf{n} \\ &= \sqrt{\frac{2E_s}{T_s}\frac{UN_c}{\gamma}}\mathbf{M}\left(\mathbf{M}^T\mathbf{d} + \tau\mathbf{l}\right) + \mathbf{n} \\ &= \sqrt{\frac{2E_s}{T_s}\frac{UN_c}{\gamma}}\left(\mathbf{d} + \tau\mathbf{M}\mathbf{l}\right) + \mathbf{n}.\end{aligned} \tag{28}$$

The interleaved perturbation vector $\tau\mathbf{Ml}$ is removed at each user by modulo operation, as SC-TDTHP. Each user can obtain the desired symbol block owing to the rearrangement of Eq. (21). Note that the perturbation vector search of Eq. (18) is performed replacing d_i and L_{ij} to the i(=0∼$UN_c \times 1$)-th element d''_i in $\mathbf{d}''$ and L''_{ij}, respectively.

4. Computer Simulation Results

Computer simulation condition is summarized in Table 1.

Table 1 Computer simulation condition.

Transmitter & Receiver	Data modulation	QPSK
	Block size	N_c=64
	CP length	N_g=8
	No. of transmit antennas	N_T=4
	No. of users	U=4
	No. of candidates of each component in a perturbation vector	K=9
	No. of paths kept in each stage	M=1~50
	Channel estimation	Ideal
Channel model	Fading	Frequency-selective block Rayleigh
	Power delay profile	8-path uniform
	Time delay of λ-th path	τ_λ=λ symbols

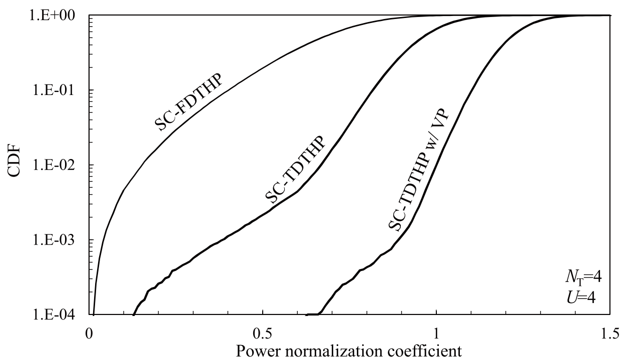

Fig. 5 CDF of power normalization coefficient.

A BS having N_T=4 transmit antennas communicates with U=4 users simultaneously. The channels are characterized as frequency-selective block Rayleigh fading, and each channel has Λ=8-path with uniform power delay profile. We assume that the channels do not have any correlation among users and paths. We also assume the BS can ideally obtain the CSI between the BS's transmit antennas and each user's received antenna. In SC-TDTHP w/VP and SC-VP, a perturbation vector for each modulated symbol is searched in −1, 0, +1 about each of real and imaginary parts, thereby K=9. Only zero-forcing (ZF) based precoding is studied in this paper.

Figure 5 plots the cumulative distribution function (CDF) of the power normalization coefficient $\sqrt{UN_c/\gamma}$ in SC-TDTHP and SC-TDTHP w/VP when M=50. The CDF of the power normalization coefficient in SC-FDTHP is also plotted in Fig. 5 for comparison. It can be seen from Fig. 5 that the CDF in SC-TDTHP has a better distribution than SC-FDTHP. This improvement implies that modulo operation in SC-TDTHP can suppress the signal variance increase caused by IUI/ISI pre-removal while that in SC-FDTHP is capable of suppressing the signal variance increase caused only by IUI pre-removal.

SC-TDTHP w/VP, SC-TDTHP, and SC-FDTHP are compared below. It can be seen from Fig. 5 that SC-TDTHP w/VP is likely to have the largest power normalization coefficient among these 3 schemes. The larger the power normalization coefficient is, the larger the received SNR is (this

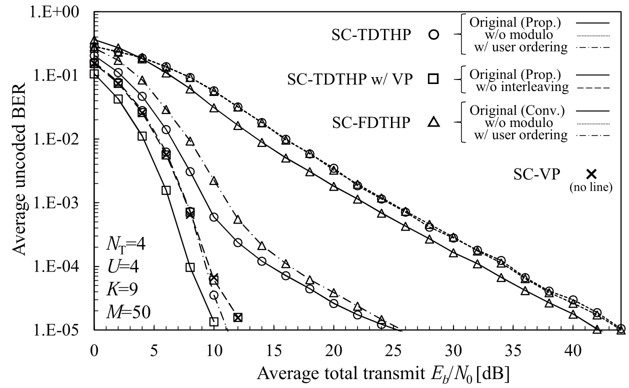

Fig. 6 Average BER performance (uncoded case).

can be understood from Eqs. (13) and (28)). Thus, SC-TDTHP w/VP can be considered to be the best among three schemes. SC-TDTHP w/VP applies perturbation vector search and interleaving/de-interleaving while SC-TDTHP applies modulo operation. Therefore, it can be said that a near-optimal perturbation vector can better suppress the signal variance increase caused by IUI/ISI pre-removal than modulo operation.

Figure 6 plots the uncoded BER performance of SC-TDTHP as a function of the average transmit bit energy-to-noise power spectral density ratio (E_b/N_0). To discuss the effects of user ordering and modulo operation on the BER performance of SC-TDTHP, the BER performances of SC-TDTHP w/user ordering and SC-TDTHP w/o modulo operation are also plotted in Fig. 6. In the user ordering, after performing precoding U! times about all order combinations of users, the BS transmits the symbol blocks when the power normalization coefficient is maximum. Figure 6 also plots the uncoded BER performances of SC-TDTHP w/VP and that w/o interleaving when M=50, which is the number of paths kept in each stage. SC-FDTHP, SC-FDTHP w/user ordering, SC-FDTHP w/o modulo operation, and SC-VP when M=50 are compared in Fig. 6. It is seen from Fig. 6 that SC-TDTHP achieves better BER performance than SC-FDTHP due to the improvement of CDF of the power normalization coefficient shown in Fig. 5. Figure 6 also proves that modulo operation in SC-TDTHP suppress the signal variance increase more than that in SC-FDTHP.

However, Fig. 6 shows that BER performance of SC-TDTHP is worse than that of SC-VP when M=50. Note that perturbation vector search is better method for suppressing the signal variance increase than modulo operation, excluding increase of computational complexity. Thus, SC-TDTHP w/VP, which applies perturbation vector search instead of modulo operation, can significantly improve the BER performance compared to SC-TDTHP. In addition, the performance of SC-TDTHP w/VP is better than that of SC-VP. The interleaving brings in the improvement since SC-TDTHP w/o interleaving achieves the same BER performance as SC-VP. The accuracy of M algorithm becomes higher by the interleaving and a nearer-optimal perturbation

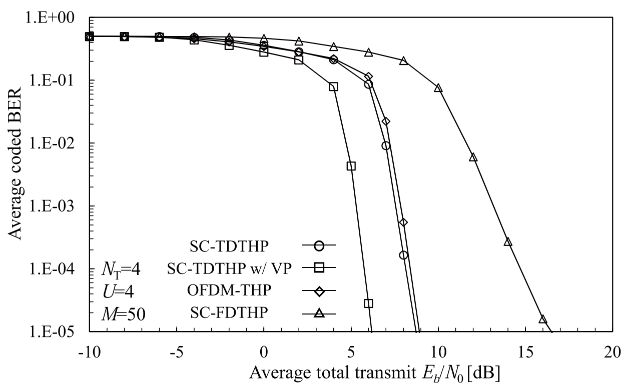

Fig. 7 Average BER performance (turbo coded case).

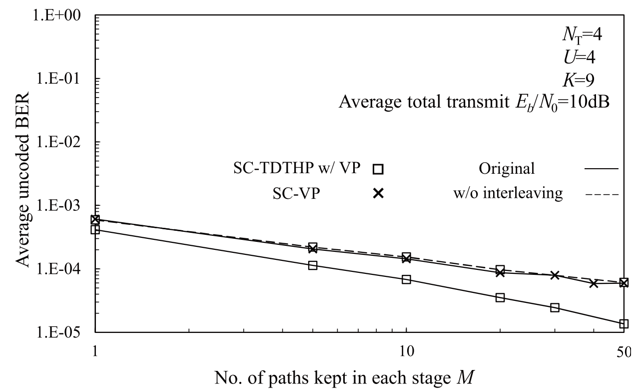

Fig. 8 Average BER as a function of M.

vector is searched.

It is also seen from Fig. 6 that the user ordering can reduce the required E_b/N_0 to achieve BER=10^{-5} by about 15 dB in SC-TDTHP and about 16 dB in SC-FDTHP. The improvement of SC-TDTHP caused by the user ordering is almost the same as that of SC-FDTHP. Thus, it is presumed that some kinds of ordering methods for THP (e.g. [13]) bring in as much improvement effect to proposed SC-TDTHP as SC-FDTHP.

Figure 7 plots the turbo coded BER performances of SC-TDTHP and SC-TDTHP w/VP when M=50 as a function of the average transmit E_b/N_0. Turbo encoder with coding rate 1/2 using two (13,15) recursive systematic convolutional (RSC) encoders, S-random interleaver/de-interleaver as the inner interleaver, 32×32 block interleaver/de-interleaver as the channel interleaver, and log maximum a *posteriori* probability (MAP) turbo decoding with 8 iterations are assumed [19]. The codeword length is 512 bits. Those of SC-FDTHP and OFDM-THP are compared in Fig. 7. In OFDM-THP, the BS applies the original THP and FDE at each subcarrier. Figure 7 shows that SC-TDTHP provides better BER performance than SC-FDTHP in applying turbo code as well. It is also shown in Fig. 7 that SC-TDTHP achieves slightly better BER performance than OFDM-THP. Both suppress the signal variance increase caused by the all interference (IUI/ISI in SC-TDTHP, IUI in OFDM-THP) pre-removal. SC-TDTHP obtains high frequency diversity gain while OFDM-THP obtains high coding gain. However, both can achieve more improvement by applying minimum mean square error (MMSE) based precoding, which maximizes signal-to-interference-plus-noise power ratio (SINR). OFDM-THP balances IUI with noise while SC-TDTHP does IUI/ISI with noise. Thus, we expect that the latter is more flexible and can obtain more improvement than the former. In this paper, ZF based precoding is only considered. MMSE based precoding is left as our future study. Figure 7 also shows that SC-TDTHP w/VP provides better BER performance than SC-TDTHP also in the coded case.

Figure 8 plots the average BERs of SC-TDTHP w/VP and that w/o interleaving as a function of M when the average transmit E_b/N_0=10 dB. For comparison, Fig. 8 also plots that of SC-VP. Increasing the number M of paths kept in each stage can find a nearer-optimal perturbation vector, and consequently improves the BER. The improvement by increasing M in SC-TDTHP w/VP is larger than that in SC-VP, due to interleaving. When M increases from 1 to 50, the BER of SC-TDTHP w/VP improves to about 1/30 while that of SC-VP improves to about 1/10.

5. Computational Complexity

This section compares the computational complexity. In this paper, the number of complex multiplications at the transmitter is compared as the computational complexity for the following reasons. (a) The receiver structure is simple and the computational complexity at a receiver is negligible compared to that at a transmitter. (b) One complex multiplication requires not less than three times as many as the computational complexity of one complex addition. Incidentally, one complex multiplication contains two real additions and four real multiplications while one complex addition is calculated by two real additions. (c) Comparison operations can be reduced by appropriate algorithms. Table 2 shows the number of complex multiplications at the transmitter in SC-TDTHP, SC-TDTHP w/VP, SC-FDTHP, and SC-VP. a is the minimum integer satisfied with $M \leq K^a$.

Compared between SC-TDTHP and SC-TDTHP w/VP, precoding matrix calculation and multiplication are the same processing. However, SC-TDTHP w/VP applies perturbation vector search using M algorithm. SC-TDTHP w/VP requires more computational complexity than SC-TDTHP due to the search.

SC-VP uses $N_T \times U$ frequency-domain precoding matrices, hence the number of complex multiplications for precoding matrix calculation and multiplication of SC-VP is smaller than those of SC-TDTHP and SC-TDTHP w/VP. However, SC-VP requires QR decomposition proportional to N_c^3. The computational complexity for perturbation vector search in SC-TDTHP w/VP is less than that in SC-VP since the equivalent precoding matrix in the former is a sparse matrix. Thus, SC-TDTHP and SC-TDTHP w/VP requires the smaller number of complex multiplications than

Table 2 Number of complex multiplications at BS.

	SC-TDTHP	SC-TDTHP w/ VP	SC-FDTHP	SC-VP
Precoding matrix calc.	$U^2N_TN_c^3$		$U^2N_TN_c$	$2U^2(U+N_T)N_c$
Time-domain equivalent precoding matrix calc.				$UN_TN_c^2$
QR decomposition				$U^2N_TN_c^3$
IUI or IUI/ISI calc.	$(UN_c-1)\times UN_c/2$	$\Omega-MKU^2\times(N_c-2\Lambda+2)\times(N_c-2\Lambda+1)/2$	$(U-1)UN_c/2$	
Perturbation vector search				$\{K-(a+1)K^{a+1}+aK^{a+2}\}/(K-1)^2+\{MK(UN_c+a+1)\times(UN_c-a)/2\}:=\Omega$
Precoding matrix multiplication	$UN_TN_c^2$		UN_TN_c	
DFT			$2UN_c^2$	UN_c^2
IDFT			$(N_T+U)N_c^2$	$N_TN_c^2$

SC-VP.

The required number of complex multiplications is proportional to N_c^3 for both SC-TDTHP and SC-TDTHP w/VP while it is proportional to N_c^2 for SC-FDTHP. The total numbers of complex multiplications in SC-TDTHP and SC-TDTHP w/VP are larger than that in SC-FDTHP. For example, assuming the computer simulation condition shown in Table 1 and M=50, we can show from Table 2 that SC-TDTHP requires complex multiplications of approximately 3/4, 240 times, and 1/2 than those in SC-TDTHP w/VP, SC-FDTHP, and SC-VP, respectively.

6. Conclusion

In this paper, we proposed SC-TDTHP, where THP preremoves ISI as well as IUI, for SC-MU-MIMO downlink. For further improvement, we also proposed SC-TDTHP w/VP, where perturbation vector search instead of modulo operation is performed at the BS transmitter. By computer simulation, we showed that SC-TDTHP achieves better BER performance than SC-FDTHP and that SC-TDTHP w/VP achieves better BER performance than SC-VP. A computation complexity comparison showed that SC-TDTHP and SC-TDTHP w/VP incur higher computational complexity than SC-FDTHP, but lower than SC-VP. For further improvement, we will study MMSE based SC-TDTHP. Theoretical analysis, the impact of channel estimation error, and reducing the computational complexity for larger block size are our important future topics. In this paper, QPSK data modulation was considered and the peak-to-average power ratio (PAPR) of the transmit signal was not considered. Both of SC-TDTHP and SC-TDTHP w/VP may increase the PAPR of transmit signal. PAPR increase is more pronounced when higher-level modulation is used. Therefore, the performance evaluation of SC-TDTHP and the PAPR of transmit signal when using higher-level modulations are also left as our important future study.

References

[1] Q.H. Spencer, C.B. Peel, A.L. Swindlehurst, and M. Haardt, "An introduction to the multi-user MIMO downlink," IEEE Commun. Mag., vol.42, no.10, pp.60–67, Oct. 2004.

[2] D. Gesbert, M. Kountouris, R.H. Heath, Jr., C.-B. Chae, and T. Salzer, "Shifting the MEMO paradigm," IEEE Signal Process. Mag., vol.24, no.5, pp.36–46, Sept. 2007.

[3] C.B. Peel, B.M. Hochwald, and A.L. Swindlehurst, "A vector-perturbation technique for near-capacity multiantenna multiuser communication-Part I: Channel inversion and Regularization," IEEE Trans. Commun., vol.53, no.1, pp.195–202, Jan. 2005.

[4] Q.H. Spencer, A.L. Swindlehurst, and M. Haardt, "Zero-forcing methods for downlink spatial multiplexing in multiuser MIMO channels," IEEE Trans. Signal Process., vol.52, no.2, pp.461–471, Feb. 2004.

[5] G. Ginis and J.M. Cioffi, "A multi-user precoding scheme achieving crosstalk cancellation with application to DSL systems," Conference Record of the Thirty-Fourth Asilomar Conference on Signals, Systems and Computers, pp.1627–1631, 2000.

[6] C.B. Peel, B.M. Hochwald, and A.L. Swindlehurst, "A vector-perturbation technique for near-capacity multiantenna multiuser communication-Part I: Channel inversion and regularization," IEEE Trans. Commun., vol.53, no.1, pp.195–202, March 2005.

[7] M. Itagaki, K. Takeda, and F. Adachi, "Frequency-domain QR-M-MLD block signal detection for single-carrier multi-user MIMO uplink," Proc. 2010 2nd IEEE InternationalConference on Network Infrastructure and Digital Content, pp.687–691, 2010.

[8] T. Yamamoto, K. Adachi, S. Sun, and F. Adachi, "Recursive QR packet combining for uplink single-carrier multi-user MIMO HARQ using near ML detection," Proc. 2012 8th International Wireless Communications and Mobile Computing Conference (IWCMC), pp.407–412, 2012.

[9] B. Deepa and P.S. Reddy, "Comparison of bit error rate and signal to noise ratio for multi-user MIMO wireless applications," International Journal of Innovation Technology and Exploring Engineering (IJITEE), vol.3, no.3, pp.52–55, Aug. 2013.

[10] C. Degen and L. Brühl, "Linear and successive predistortion in the frequency domain: Performance evaluation in SDMA systems," Proc. IEEE Wireless Communications and Networking Conference, pp.718–723, 2005.

[11] S. Yoshioka, S. Kumagai, and F. Adachi, "Vector perturbation for single-carrier MU-MIMO downlink," Proc. 2014 IEEE International Conference on Communication Systems, pp.507–511, 2014.

[12] J. Zhang and K.J. Kim, "Near-capacity MIMO multiuser precoding with QRD-M algorithm," Conference Record of the Thirty-Ninth Asilomar Conference onSignals, Systems and Computers, pp.1498–1502, 2005.

[13] J. Liu and W. Kizymień, "Improved Tomlinson-Harashima precoding for the downlink of multi-user MIMO systems," Can. J. Electr. Comput. Eng., vol.32, no.3, pp.133–144, 2007.

[14] F. Adachi, H. Tomeba, and K. Takeda, "Frequency-domain equalization for broadband single-carrier multiple access," IEICE Trans. Commun., vol.E92-B, no.5, pp.1441–1456, May 2009.

[15] D. Falconer, S.L. Ariyavisitakul, A. Benyamin-Seeyar, and B. Eidson, "Frequency domain equalization for single-carrier broadband wireless systems," IEEE Commun. Mag., vol.40, no.4, pp.58–66, April 2002.

[16] H. Moroga, T. Yamamoto, and F. Adachi, "Overlap QRM-ML block signal detection for single-carrier transmission without CP insertion," Proc. 2012 IEEE 75th Vehicular Technology Conference (VTC Spring), pp.1–5, 2012.

[17] H. Moroga, T. Yamamoto, and F. Adachi, "Iterative overlap TD-QR-M-ML block signal detection for single-carrier transmission without CP insertion," Proc. 2012 IEEE Vehicular Technology Conference (VTC Fall), pp.1–5, 2012.

[18] C.C. Paige and M.A. Saunders, "Solution of sparse indefinite systems of linear equations," SIAM J. Numer. Anal., vol.12, no.4, pp.617–629, Sept. 1975.
[19] D. Garg and F. Adachi, "Application of rate compatible punctured turbo coded hybrid ARQ to MC-CDMA mobile radio," ETRI J., vol.26, no.5, pp.405–412, Oct. 2004.

Appendix:

Perfect CSI between the BS's transmit antennas and each user's received antenna is assumed to be available at BS.

A.1 SC-FDTHP

SC-FDTHP uses precoding in frequency-domain since LQ decomposition [18] is applied to the frequency domain channel matrix. IUI is pre-removed by successive subtraction in frequency-domain while modulo operation is applied in time-domain. Since the signal at each subcarrier obtained by discrete Fourier transform (DFT) has fairly a large number of levels, modulo operation cannot be applied. ISI is pre-removed by transmit FDE.

After some manipulations, we obtain the $N_T \times 1$ frequency-domain transmit symbol vector $\mathbf{S}_I(k)$ as

$$\mathbf{S}_I(k) = \sqrt{\frac{UN_c}{\gamma_I}}\mathbf{F}(k)\mathbf{W}(k)\mathbf{X}_I(k), \tag{A$\cdot$1}$$

$$\gamma_I = \sum_{k=0}^{N_c-1} \|\mathbf{F}(k)\mathbf{W}(k)\mathbf{X}_I(k)\|^2, \tag{A$\cdot$2}$$

where $\mathbf{F}(k)$ and $\mathbf{W}(k)$ are the precoding matrix and the transmit FDE weight, respectively. $\mathbf{X}_I(k)$ is the symbol vector after IUI subtraction and modulo operation.

The received symbol vector $\mathbf{r}_I(t)$=$[r_{I,0}(t)\ldots r_{I,U-1}(t)]^T$ is given as

$$\mathbf{r}_I(t) = \sqrt{\frac{2E_s}{T_s}\frac{UN_c}{\gamma_I}}(\mathbf{d}_I(t) + \tau\mathbf{z}_I(t)) + \mathbf{n}_I(t), \tag{A$\cdot$3}$$

where $\mathbf{d}_I(t)$, $\mathbf{z}_I(t)$, and $\mathbf{n}_I(t)$ are the $U \times 1$ all users' symbols vector, the $U \times 1$ modulo component vector, and the $U \times 1$ noise vector. When turbo coding and QPSK are used, the bit LLR is computed for the b(=0 or 1)-th bit as

$$\mathrm{LLR}_{I,u}(t,b) = \frac{1}{2\sigma^2}\left(\left|r_{I,u}(t) - \sqrt{\frac{2E_s}{T_s}\frac{UN_c}{\gamma_I}}\xi_{I,0,\min}\right|^2 - \left|r_{I,u}(t) - \sqrt{\frac{2E_s}{T_s}\frac{UN_c}{\gamma_I}}\xi_{I,1,\min}\right|^2\right). \tag{A$\cdot$4}$$

where $\xi_{I,0,\min}$ or $\xi_{I,1,\min}$ are the candidate symbols having the b-th bit=0 and 1, respectively, which give the minimum Euclidean distance from $r_{I,u}(t)$.

A.2 OFDM-THP

OFDM-THP uses the same precoding matrix and transmit FDE weight as those of SC-FDTHP. Modulo operation as well as successive IUI subtraction and transmit FDE is applied in frequency-domain.

After some manipulations, we obtain the $N_T \times 1$ frequency-domain transmit symbol vector $\mathbf{S}_{II}(k)$ as

$$\mathbf{S}_{II}(k) = \sqrt{\frac{U}{\gamma_{II}(k)}}\mathbf{F}(k)\mathbf{W}(k)\mathbf{X}_{II}(k), \tag{A$\cdot$5}$$

$$\gamma_{II}(k) = \|\mathbf{F}(k)\mathbf{W}(k)\mathbf{X}_{II}(k)\|^2, \tag{A$\cdot$6}$$

where $\mathbf{X}_{II}(k)$ is the symbol vector after IUI subtraction and modulo operation.

The received symbol vector $\mathbf{r}_{II}(k) = [r_{II,0}(k) \ldots r_{II,U-1}(k)]^T$ at the k-th subcarrier is given as

$$\mathbf{r}_{II}(k) = \sqrt{\frac{2E_s}{T_s}\frac{U}{\gamma_{II}(k)}}(\mathbf{d}_{II}(k) + \tau\mathbf{Z}_{II}(k)) + \mathbf{N}_{II}(k), \tag{A$\cdot$7}$$

where $\mathbf{d}_{II}(k)$, $\mathbf{Z}_{II}(k)$, and $\mathbf{N}_{II}(k)$ are the $U \times 1$ all users' symbols vector, the $U \times 1$ modulo component vector, and the $U \times 1$ noise vector. When turbo coding and QPSK are used, the bit LLR is computed for the b(=0 or 1)-th bit as

$$\mathrm{LLR}_{II,u}(k,b) = \frac{1}{2\sigma^2}\left(\left|r_{II,u}(k) - \sqrt{\frac{2E_s}{T_s}\frac{U}{\gamma_{II}(k)}}\xi_{II,0,\min}\right|^2 - \left|r_{II,u}(k) - \sqrt{\frac{2E_s}{T_s}\frac{U}{\gamma_{II}(k)}}\xi_{II,1,\min}\right|^2\right). \tag{A$\cdot$8}$$

where $\xi_{II,0,\min}$ or $\xi_{II,1,\min}$ are the candidate symbols having the b-th bit=0 and 1, respectively, which give the minimum Euclidean distance from $r_{II,u}(k)$.

Shohei Yoshioka received his B.E. degree in Information and Intelligent Systems in 2013 from Tohoku University, Sendai, Japan. Currently, he is a graduate student at the Department of Communications Engineering, Tohoku University. His research interests include channel equalization and multi-user MIMO (MU-MIMO) transmission techniques for mobile communication systems.

Shinya Kumagai received his B.E. degree in Information and Intelligent Systems in 2011 and M.E. degree in Electrical and Communications engineering in 2013, respectively, from Tohoku University, Sendai, Japan. Currently, he is a Japan Society for the Promotion of Science (JSPS) research fellow, studying toward his Ph.D. degree at the Department of Communications Engineering, Graduate School of Engineering, Tohoku University. His research interests include channel equalization and multiple-input multiple-output (MIMO) transmission techniques for mobile communication systems. He was a recipient of the 2012 IEICE RCS (Radio Communication Systems) Outstanding Research Award.

Fumiyuki Adachi received the B.S. and Dr. Eng. degrees in electrical engineering from Tohoku University, Sendai, Japan, in 1973 and 1984, respectively. In April 1973, he joined the Electrical Communications Laboratories of Nippon Telegraph & Telephone Corporation (now NTT) and conducted various types of research related to digital cellular mobile communications. From July 1992 to December 1999, he was with NTT Mobile Communications Network, Inc. (now NTT DoCoMo, Inc.), where he led a research group on wideband/broadband CDMA wireless access for IMT-2000 and beyond. Since January 2000, he has been with Tohoku University, Sendai, Japan, where he is a Professor of Communications Engineering at the Graduate School of Engineering. In 2011, he was appointed a Distinguished Professor. His research interests are in the areas of wireless signal processing and networking including broadband wireless access, equalization, transmit/receive antenna diversity, MIMO, adaptive transmission, and channel coding, etc. From October 1984 to September 1985, he was a United Kingdom SERC Visiting Research Fellow in the Department of Electrical Engineering and Electronics at Liverpool University. Dr. Adachi is an IEEE fellow and a VTS Distinguished Lecturer for 2011 to 2013. He was a co-recipient of the IEEE Vehicular Technology Transactions best paper of the year award 1980 and again 1990 and also a recipient of Avant Garde award 2000. He was a recipient of Thomson Scientific Research Front Award 2004 and Ericsson Telecommunications Award 2008, Telecom System Technology Award 2009, and Prime Minister Invention Prize 2010.